

Effective control of dental aerosols and splatters via commercial extraoral suction and an innovative design with annular air curtain

C.T. Wang¹, G. Yang², Christopher Y.H. Chao^{2,3}, S.C. Fu^{2*}

¹ *Department of Civil and Environmental Engineering, The Hong Kong Polytechnic University, Hong Kong, China*

² *Department of Building Environment and Energy Engineering, The Hong Kong Polytechnic University, Hong Kong, China*

³ *Department of Mechanical Engineering, The Hong Kong Polytechnic University, Hong Kong, China*

* Corresponding author(s):

S.C. Fu, Department of Building Environment and Energy Engineering, The Hong Kong Polytechnic University, Hung Hom, Hong Kong. Email: schung.fu@polyu.edu.hk

Abstract

Dental professionals in dental clinics are more likely to be infected by dental aerosols and splatters (splatter: $>50\ \mu\text{m}$ in diameter). The extraoral suction (EOS) device has long been developed but has not been widely used to remove dental aerosols in dentistry because its performance varies widely. An innovative new design with an annular air curtain (EOS-AAC) was proposed in this work. The performance of both the commercial EOS and the new EOS-AAC design in removing dental aerosols and splatters was evaluated by numerical simulations. The new design can confine and guide the released dental aerosols and splatters toward the suction head. The new design for dental surgeries can create a large separation distance of 30

cm from the patient's mouth. The aerosol and splatter removal ratios were up to 98% by the innovative EOS-AAC design at a low central suction velocity of 6-9 m/s (Flow rate: 1.5-2.25 m³/min). It is a significant improvement over currently available EOS devices with an aerosol removal ratio of 10% and splatter removal ratio of less than 1% at a distance of 30 cm. The new design can also be promoted to different indoor scenarios to remove contaminants.

Keywords: Infection control, Air curtain, Extraoral scavenger, Indoor air quality, COVID-19

Introduction

The generation of aerosols during dental procedures has long been recognized in dental practice.^{1, 2} There have been increasing concerns about the exposure of dental professionals and patients to aerosols in dental hospitals and the potential transmission of infectious diseases such as *M. tuberculosis* and severe acute respiratory syndrome (SARS).³⁻⁶ The COVID-19 pandemic caused by the novel coronavirus has raised significant concerns about the virus transmission via aerosolized saliva in dental care settings.^{7, 8} Given the high risk of virus transmission, dental hospitals, and clinics were temporarily suspended at the beginning of COVID-19.^{9, 10} Therefore, practical and robust infection control measures are necessary to mitigate the spread of the SARS-CoV-2 virus and other emerging infectious pathogens in dental clinics.

Large amounts of aerosols and splatters (splatter: > 50 µm in diameter) are generated from the oral cavity during dental procedures.^{4-6, 11, 12} Field measurements confirmed that the concentration of bacterial aerosols peaks following dental procedures.¹³⁻¹⁵ The areas up to 11 m away from dental patients could still experience increased bacterial aerosols.¹⁶ The surface contamination by bacterial aerosols and splatters was high within 1.5-2 m of patients.^{1, 17} The contamination was detectable at 4 m away from patients.⁹ The concentration of SARS-CoV-2

in a patient's saliva could be up to 10^{9-10} copies/mL,^{18, 19} indicating the high risk of infection by saliva aerosols. Three transmission routes of SARS-CoV-2 exist, similar to other respiratory diseases such as Influenza, SARS-CoV-1, and MERS-CoV, that is, airborne, droplet, and contact.²⁰⁻²³ Airborne aerosols can deposit in the lower respiratory tracts by inhalation and cause infections.^{24, 25} Large droplets could quickly spray on mucous membranes due to large inertia and cause infection.²⁶ The deposited aerosols and splatters can also be transferred to mucous membranes by touching contaminated surfaces, that is, the indirect contact route or fomite route.²⁷⁻²⁹ During dental surgeries, dentist providers are in close contact with patients, indicating the simultaneous exposure to aerosols, droplets, and fomites.

Many precautions and control measures were recommended for the COVID-19 pandemic.^{30, 31} For example, rubber dam isolation for patients, antiseptic mouth rinses before dental procedures, evaluation of patients by questionnaire, personal protective measures for dental professionals, and standard precautions should be followed by dental providers to mitigate disease transmission. A high-volume evacuator (i.e., intraoral suction) is usually put inside the oral cavity to remove dental aerosols immediately. A dental assistant is generally necessary to hold the evacuator. Aerosol reduction by intraoral suction is at an extensive range of 20-100%,³²⁻³⁸ depending on whether the suction tube is in the ideal position. Among different control measures, local exhaust ventilation (i.e., extraoral suction EOS) has long been proposed but is not widely used to remove dental aerosols. The extraoral suction can remove dental aerosols from the source and does not need an additional dental assistant to hold compared with the intraoral suction (i.e., high-volume evacuator). However, the actual reduction ratios vary in an extensive range from 20% to 90%, as indicated in previous studies.^{32-34, 39-41} For the EOS design, the separation distance with the patient's mouth and the flow rate of the suction are important for removing dental aerosols, which may be the reason for the large discrepancy in

EOS performance in references. However, the effect of the separation distance and flow rate on dental aerosol removal remains unclear.

In recent years, air curtains have been widely investigated to block expiratory aerosols or indoor contaminants in different situations. For example, Xu et al.⁴² investigated the effectiveness of a thin, upward-blowing air curtain against coughing in an office. The air curtain can bend respiratory jets upward and reduce the person's exposure at the back. Xu et al.⁴³ further evaluated its performance in blocking the expiratory jets with different velocities, which achieved good performance. Liu et al.⁴⁴ employed square air curtains to confine cooking contaminants that were then exhausted by the suction hood without leakage. Takamure et al.⁴⁵ designed an air curtain system to protect healthcare workers in a blood collection site against infectious disease transmission, which was resistant even when the patient's arm was on the air curtain diffuser. Chen et al.⁴⁶ installed a personalized air curtain on the side wall of a consulting ward, achieving a 55%-80% reduction in exhaled pollutants. Ye et al.⁴⁷ investigated the effect of supply air velocity and angle on the performance of the air curtain on a normal consulting desk. Rosa et al.⁴⁸ developed an air curtain-sealed personal protective equipment in a dental clinic and showed good sealing performance for healthcare workers. Wei et al.⁴⁹ and Ma et al.⁵⁰ studied the wearable air curtains integrated with the helmet in an industrial setting, which can significantly reduce inhalation exposure. Wei et al.⁵¹ further studied the user's turning around and walking conditions with a helmet-based air curtain and found that the system performed well with higher air curtain flow rates. Yang et al.⁵² integrated an air curtain into the soft clothing to reduce the exposure to fine dust. These studies indicate that air curtains have excellent performance in confining the aerosols and reducing the exposures of people under proper design. However, no research has applied air curtains to dentistry to prevent dental aerosol release and protect dental personnel.

Therefore, in this work, we first evaluated the performance of traditional EOS in removing dental aerosols under various conditions and then applied the air curtain technique to the EOS device. An annular air curtain (AAC) technique was proposed for confining dental aerosols and splatters. The annular upward air curtain is created above the patient's face and centred at the mouth, serving as a virtual partition to confine and guide the aerosols and splatters toward the EOS head. Numerical simulations were employed to develop and test the new design, which can visualize the aerosol and splatter trajectories and help understand the underlying mechanism of aerosol and splatter removal. Both the traditional EOS and the new design were studied and compared. The traditional EOS has a limited ability to remove large dental splatters. The new design of EOS-AAC can be used for common dental surgeries that generate many dental aerosols, such as ultrasonic scaling, high- and low-speed drilling, and tooth polishing.

Methodology

Geometric setup of the dental clinic for numerical modeling

Field measurement was first conducted at The Prince Philip Dental Hospital (PPDH) in Hong Kong to obtain information on ventilation parameters and dental procedures. The geometric setup of the open dental surgery area in PPDH was employed for numerical modeling, as shown in Figure 1. The size of the dental clinic was $6.0 \times 4.8 \times 3.0$ m (length \times width \times height). The inlets of ventilation with a size of $0.6 \text{ m} \times 0.6 \text{ m}$ and outlets of $0.4 \text{ m} \times 1.2 \text{ m}$ were located at the ceiling, providing the mixing ventilation. The flow rate of each air diffuser on the ceiling was measured by a Balometer Capture Hood (TSI EBT731). After transferring the flow rate to the mean velocity of each diffuser, it was found that the velocity of different diffusers deviated a lot from each other, with a median value of around 0.4 m/s , which was employed in this work to consider the most common situation. One patient was lying on the dental chair in the numerical simulation domain. A dentist and a dental assistant were located on two sides of the patient. Two dental tables were located on the two sides of the dental chair. The commercial

extraoral suction (EOS, W008, free arm forte-S, Japan) was purchased by the PPDH during the pandemic as supplementary aerosol removal equipment. In this work, an EOS was set to be located between the dental table and the dental chair. The suction head was above the patient's mouth with different separation distances. The suction head has a circular shape of 10 cm in diameter with a maximum flow rate of 3 m³/min and a peak central velocity of 12 m/s at the center point (VelociCalc 9545 TSI).

The performance of the commercial EOS design was first systematically investigated. Four separation distances of 15, 20, 25, and 30 cm were investigated. The minimal separation distance between the EOS hand and patient was 15 cm for dental surgeries, as suggested by the dentists. Three flow rates (1.5, 2.25, and 3 m³/min) were studied, corresponding to the central suction velocities, V , of 6, 9, and 12 m/s.

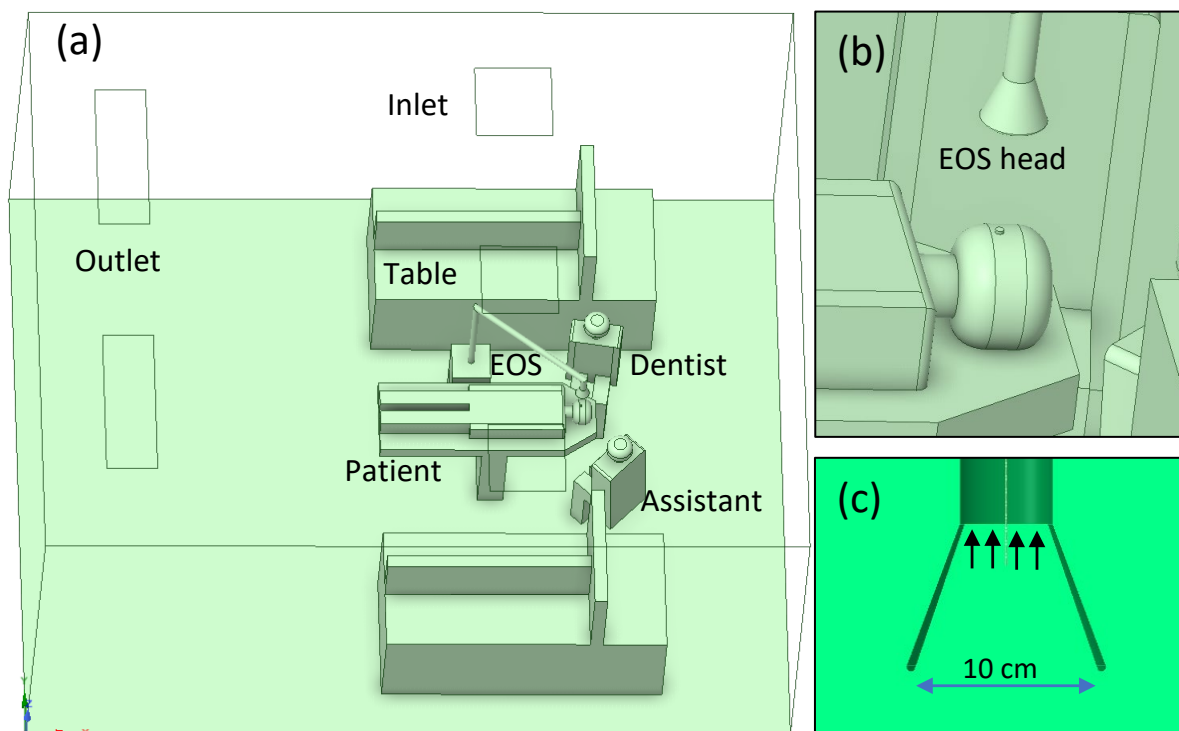


Figure 1. Geometric setup of the dental clinic for simulation. (a) overall view, (b) enlarged area of the EOS head and patient, and (c) cross-section of the EOS head.

The new design of extraoral suction with annular air curtain (EOS-AAC)

We proposed employing an AAC toward the EOS head to overcome the disadvantages of traditional extraoral suction. The AAC works as a virtual partition to prevent the leakage of aerosols and splatters but allows dentists to conduct dental procedures. The setup of the EOS-AAC design is shown in Figure 2. The EOS head has a diameter of 10 cm. The device generating AAC has an outer diameter, d , of 20 cm, which is centred at the patient's mouth and 1 cm above the mouth. The separation distance, D , was set as 30 cm. The width, w , of the annular device, was set at 1 cm. The inner thickness, h_1 , of the annular device was 0.5 cm. The relative height, h_2 , was set as 1.7 mm, determined by the distance D so airflow would point to the suction head, as shown in Figure 2b. Five AAC velocities, V_{AAC} , of 1, 2, 3, 4, and 5 m/s were tested with a separation distance of 30 cm. During dental surgeries, the wrist of the dentist or assistant and dental instrument, such as an intraoral suction tube, may be very close to the patient's mouth and interact with the AAC, affecting the EOS-AAC performance in removing dental aerosols and splatters. Therefore, the robustness analysis was conducted by putting a simulated wrist and dental instrument above the AAC inlet, as shown in Figure 2c.

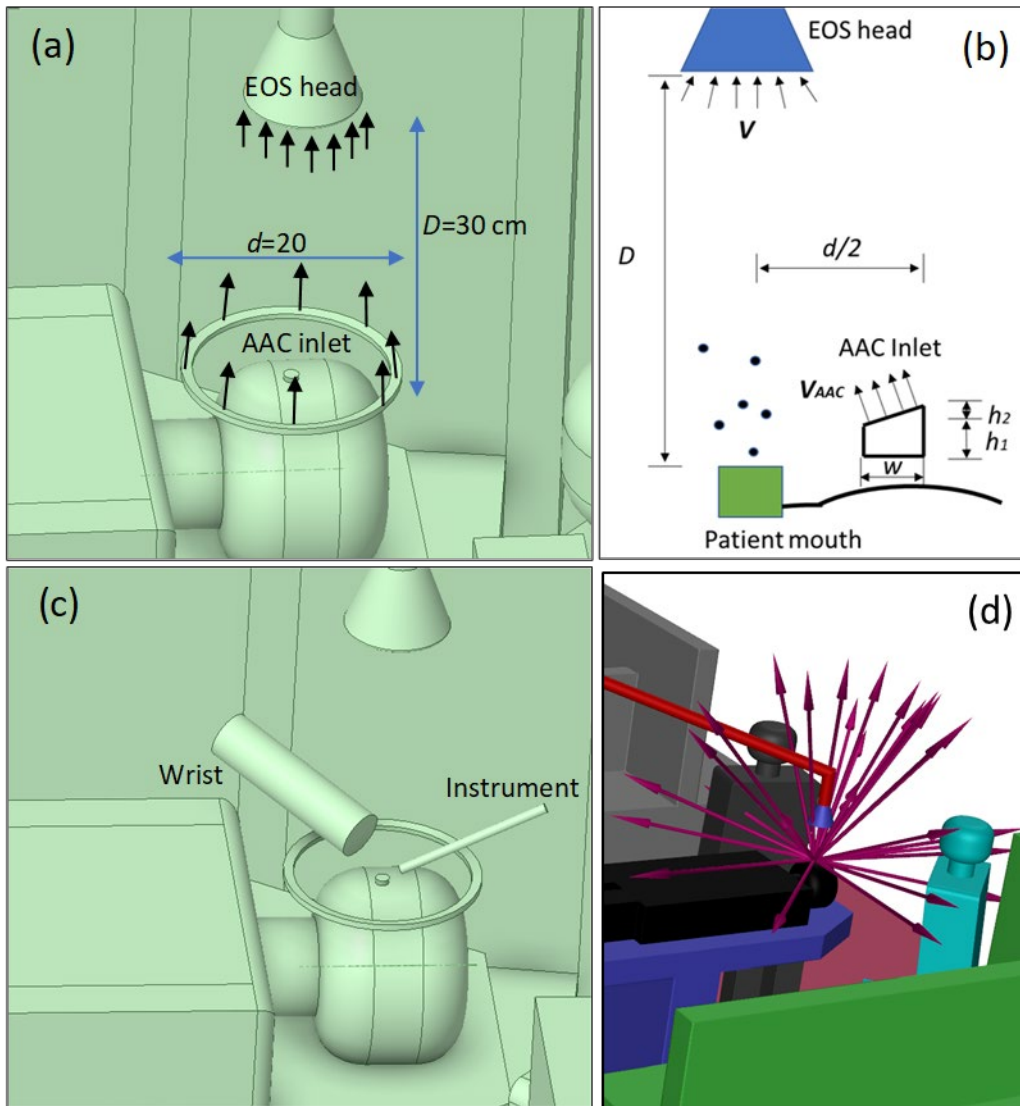


Figure 2. (a) The innovative design of the EOS-AAC for aerosol and splatter removal. (b) Schematic diagram of the cross-section of the EOS-AAC. (c) Geometry for robustness analysis of EOS-AAC with the disturbance from the simulated wrist and dental instrument with 5 cm and 1 cm diameters, respectively. (d) Releasing directions of dental aerosols and splatters in the simulations.

Numerical modelling of air phase and particle movement

ANSYS Fluent was employed to solve the Navier-Stokes equations and acquire the flow field of the air phase. The RNG $k-\varepsilon$ model, which performs well in simulating the turbulent airflow in indoor environments, was employed to solve the continuous air phase.⁵³ The energy equation

was calculated in the simulation to consider the thermal effect in the dental clinics. The SIMPLE scheme was employed for pressure-velocity coupling. The PRESTO! was used to solve the pressure equation. The second-order upwind schemes were employed to discretize the momentum, turbulent kinetic energy, turbulent dissipation rate, and energy equations. The residual of 10^{-6} for energy and residuals of 10^{-3} for continuity, velocity, turbulence, and epsilon were set as the convergence criteria. The Lagrangian discrete phase model (DPM) was employed to track particle movement. It was assumed that the airflow was not affected by the aerosols due to the small volume fraction of aerosols in the air phase. The particle-particle interaction was not considered in this work. The drag force, gravitational force, Brownian force, and lift force were considered in aerosol dispersion. The heat power of the patient and the assistant was set as 39 W/m^2 , representing a human with light activity in the office based on the ASHRAE standards. The thermal plumes of the dentist and assistant were then simulated in the dental clinic. The power of the outer wall near the dentist was set as 10 W/m^2 for a typical outer wall. The species transport model was employed to consider indoor air's water vapor content (i.e., relative humidity). The water vapor of the inlet airflow was set as 0.01042 for the relative humidity of 60% and temperature of $23 \text{ }^\circ\text{C}$.⁵⁴ The water vapor of the AAC airflow was set as 0.01107 for the relative humidity of 60% and temperature of $24 \text{ }^\circ\text{C}$, which is the typical environmental conditions in Hong Kong dental clinics. The detailed boundary conditions are summarized in Table 1.

Table 1. Setup of the boundary conditions

Items	Setup of boundary conditions
Inlet of ventilation	Temperature 23°C , relative humidity 60%, water vapor mass fraction 0.01042, DPM reflection
Outlet of ventilation	Pressure outlet, DPM exhaust

AAC inlet	Air velocity 1, 2, 3, 4, and 5 m/s, temperature 24°C, relative humidity 60%, water vapor mass fraction 0.01107, DPM reflection
Suction head	Outlet with flow rates of 1.5, 2.25, and 3 m ³ /min
Patient, dentist, and assistant	Heat flux 39 W/m ² , DPM trap
Patient mouth	Source of aerosol (diameter of 1 μm, 10 μm), splatter (50 μm, 70 μm, 100 μm), and droplet (500 μm) with velocity 3m/s, 90° cone angle, solid mass ratio of 0.6%
Mouth of the dentist and assistant	Velocity inlet -1.4 m/s, DPM exhaust
Inner walls, roof, and ground	Isothermal, DPM trap
Exterior wall	Heat flux 10 W/m ² , DPM trap

The poly-hexcore mesh was created using Fluent(meshing), the latest advanced meshing technique provided by ANSYS. The surface mesh for inlets, outlets, dentist, assistant, and patient was set as 8 mm. The surface mesh for mouths, suction head, and air curtain inlet was set as 1 mm to capture the detailed flow field. Six inflation layers were created above all the walls with the smooth transition function. The y -plus of the walls was less than 4, which fulfilled the requirement for enhanced wall treatment.⁵³ The maximum body mesh size was set as 16 mm. A body of influence with a cell size of 4 mm was created, covering the area of the patient head, EOS, and AAC to capture the reliable and fine flow features, shown in Figure 4.

Three different mesh numbers were created and compared for the mesh independent check, that is, 12.2, 27.7, and 30.7 million. The air velocity at a vertical line passing the patient's mouth was compared and shown in Figure 3. The results of the coarse mesh deviated from the other two meshes. The mean velocity of the cross sections was also compared, and the relative error was calculated, as shown in Table 2. The relative error between the medium mesh and fine mesh was less than 5%. Thus, medium mesh was employed as a balance between the accuracy and computational cost, as shown in Figure 4.

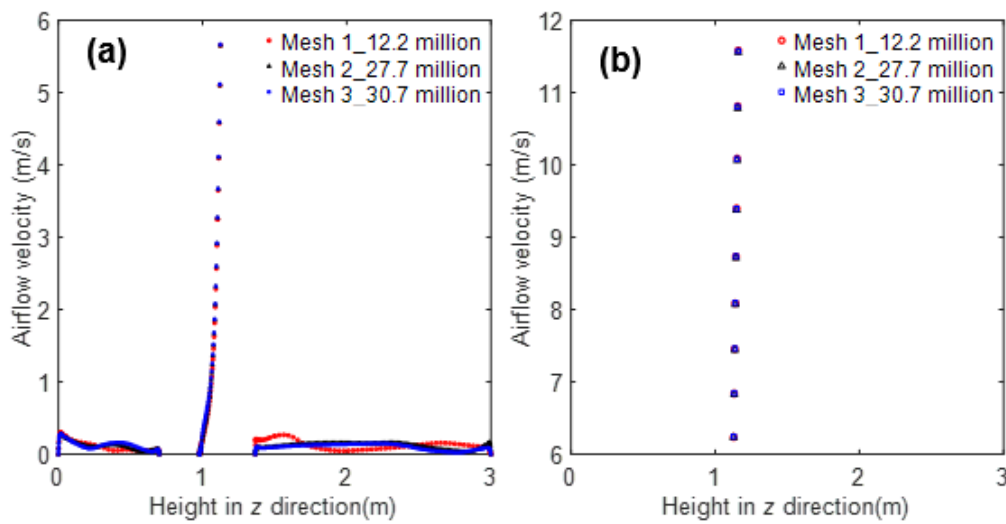


Figure 3. Comparison of air velocities for mesh independent check with three different mesh numbers. (a) The velocity range of 0-6 m/s and (b) the velocity range of 6-12 m/s. The line for comparison passes the patient's mouth, and the Z is the vertical direction.

Table 2. Mesh parameters for mech independent check

Mean velocity	12.2 million	27.7 million	30.7 million
x	0.101	0.085	0.089
Error	15.8%	4.7%	-
y	0.120	0.112	0.113
Error	6.7%	0.9%	-

z	0.092	0.085	0.083
Error	7.6%	2.4%	-

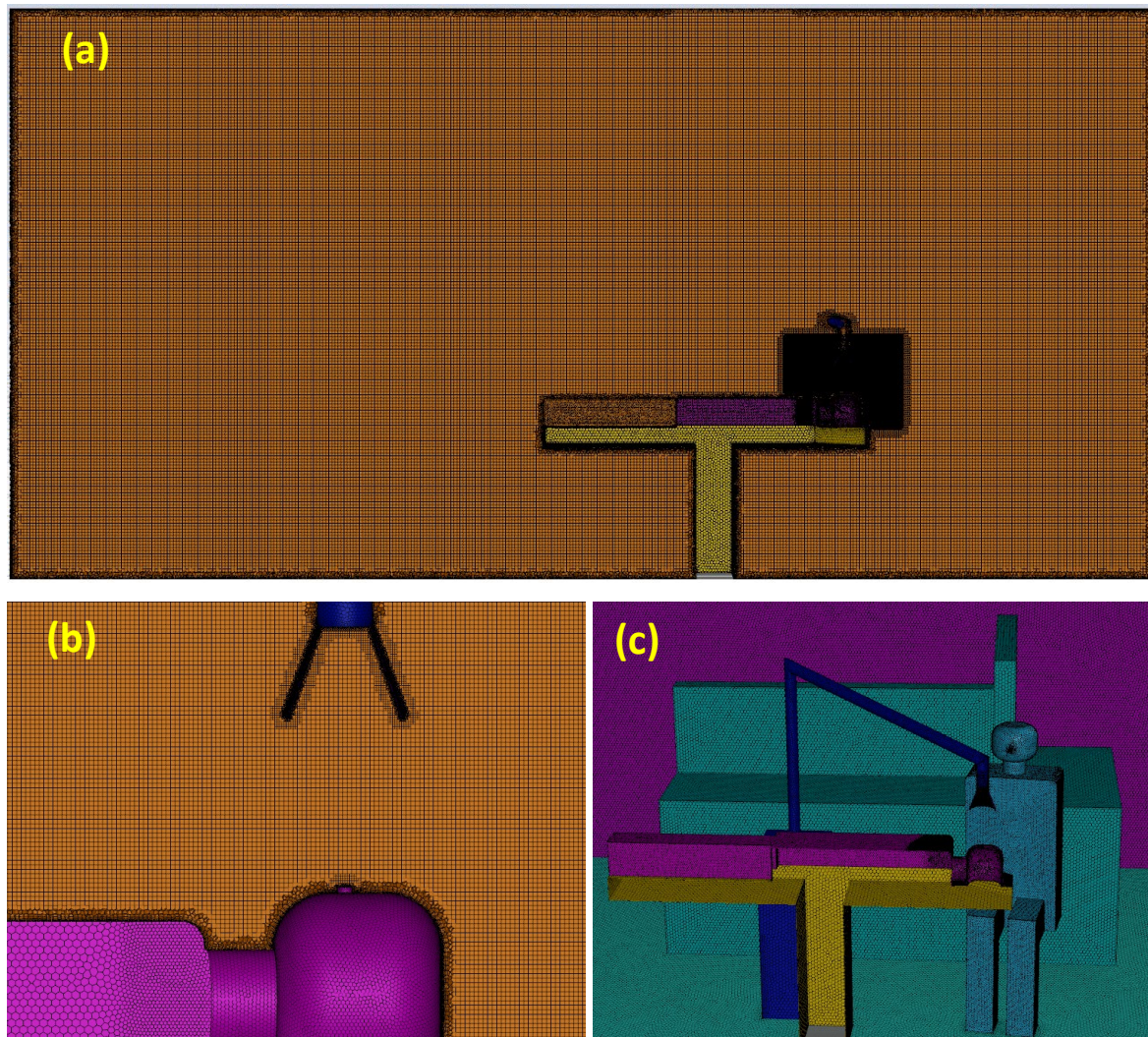


Figure 4. Poly-hexcore mesh cells in this work. (a) Body meshes in cross-section, (b) enlarged body meshes near the EOS and patient head, and (c) surface meshes of the dental clinic

Numerical setup of the dental aerosols and splatters

The PIV experiment in reference indicated that the dental aerosols were released at various directions depending on the operated tooth position, and the releasing velocity ranged from 0.5-4 m/s.⁵⁵ Therefore, in the numerical simulation, the aerosols were released from the mouth

with a full cone shape with an angle of 90° to represent the overall aerosols released in all directions during dental surgeries, as shown in Figure 2d. The releasing velocity was set as 3 m/s. Over 80% of released dental particles were smaller than 100 μm.⁵⁵ So, in this work, six different sizes were studied to cover a full range of dental particles, including 1 μm, 10 μm, 50 μm, 70 μm, 100 μm, and 500 μm, representing the dental aerosols (< 50 μm^{1,2}), splatters (50 μm - 100 μm^{1,2}), and droplets (> 100 μm).

The evaporation of aerosols and splatters was considered in this work. The dental aerosols and splatters are a mixture of saliva and cooling water. The salivary flow rate during dental surgeries ranged from 0.17 to 7.3 mL/min,^{56,57} which is around 1/10 of the cooling water flow rate of 15 to 40 mL /min.⁵⁸ The initial saliva had a solid mass ratio of around 6%,⁵⁹ and then the mixture of dental aerosols was assumed to have a solid mass ratio of 0.6%. The multi-component function in the DPM was employed to simulate the evaporation process of aerosols and splatters. The random walk model was used to consider the turbulence effect. The walls and objects in the dental clinic were set as trapping aerosols to simulate the real scenario of aerosol deposition on indoor surfaces.

The high and low-speed drilling by air turbine handpieces released more significant dental particles than others, with a particle emission rate of 10⁷ # per minute.⁶⁰ 200,000 trajectories were released and tracked for each size to give a stable removal ratio. The overall dental particle number was 1.2×10⁶ #, roughly corresponding to the particles from 10 seconds of dental surgeries. The numerical simulation can obtain the numbers of the aerosols removed by the EOS and EOS-AAC. The aerosol removal ratio was calculated as follows:

$$\text{Removal ratio} = \frac{\text{Number of removed aerosols}}{\text{Number of released aerosols}} \quad (1)$$

Validation of numerical modeling by experimental data

The experimental data from Xu et al.⁶¹ was employed to validate the air phase velocity and temperature of this work. The airflow in the work of Xu et al.⁶¹ was simulated by the identical numerical model and scheme used in this work. The computational domain (3.9×6.0×2.35 m in W×L×H) was reconstructed as shown in Figure 5, which had a comparative size with the studied dental clinic in this work. The airflow velocity and temperature profiles by numerical simulation matched reasonably well with the experimental data along the four lines in Figure 6. The comparison indicated the capability of the numerical modelling to capture the indoor airflow field.

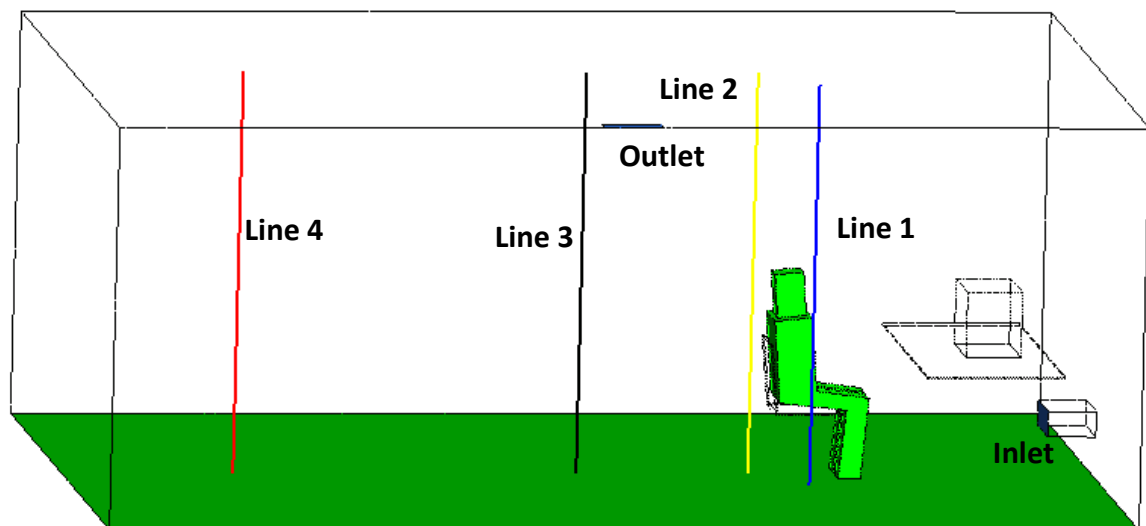


Figure 5. Computational domain for the airflow validation and the position of four lines for comparison

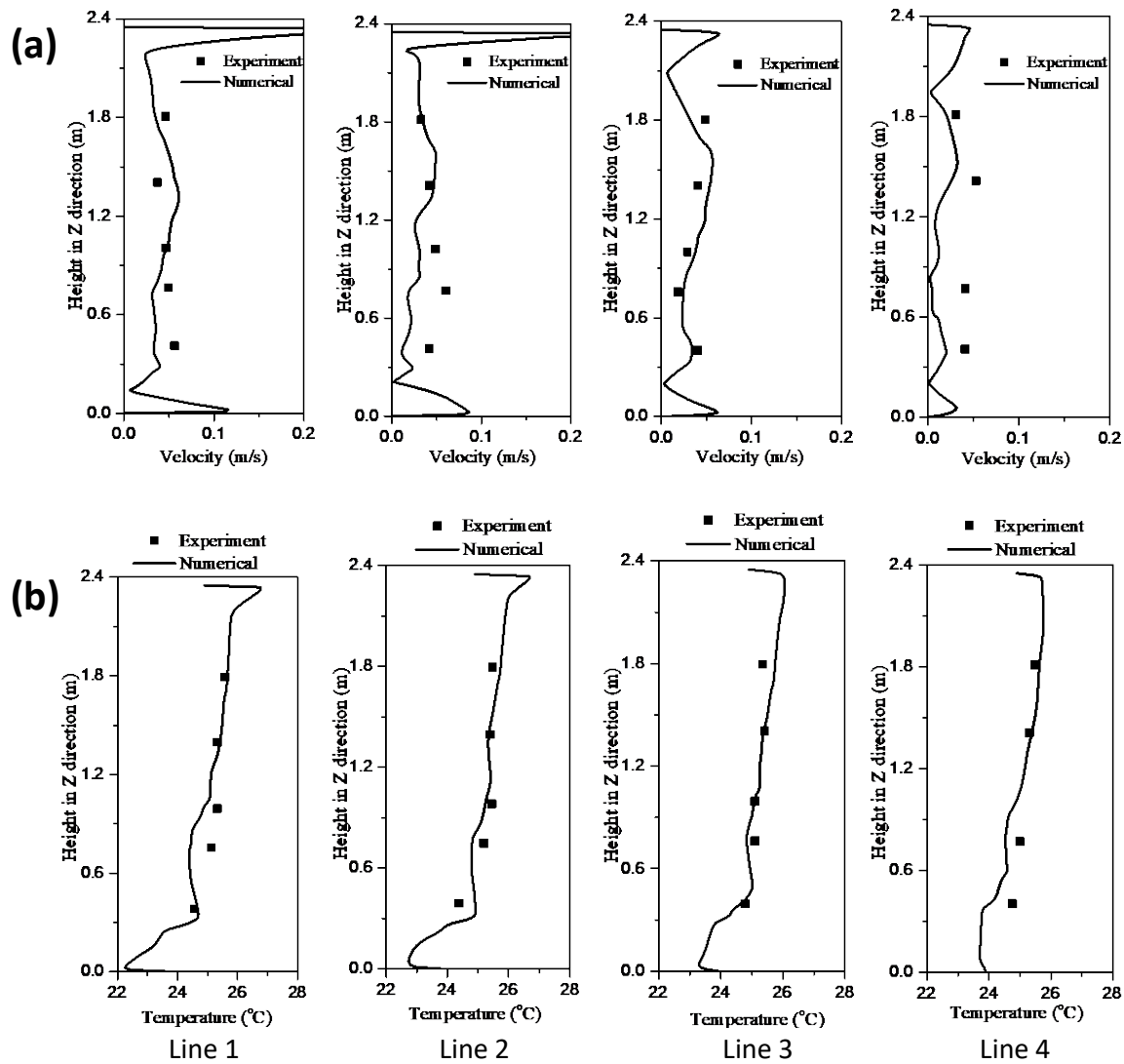


Figure 6. Comparison of numerical simulation with experimental data. (a) velocity profile and (b) temperature profile along four typical lines 1-4.

The experimental data in a reference by Xu et al.⁶² was employed to validate our numerical simulation in calculating the velocity field of an air curtain. We simulated the same experimental setup outlined in the reference using our numerical models, as shown in Figure 7a. The air curtain's initial width was 1 cm, and the initial velocities V were set as 3 m/s and 5 m/s, the same as those in the reference. The axial central velocity decay of the straight air curtain in the reference was compared with the numerical simulation, as shown in Figure 7b. The numerical model well captured the velocity decay of the air curtain, indicating the capability of simulating the air curtain.

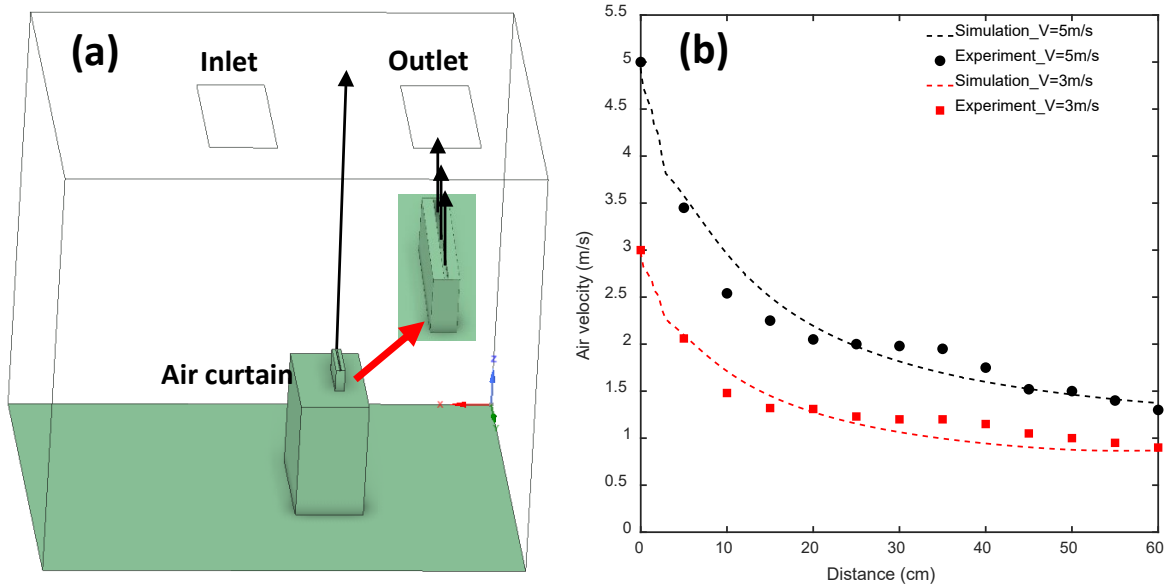


Figure 7. (a) Geometry of numerical simulation for validation and (b) comparison of velocity decay with experimental data.

Results

Performance of the EOS in removing dental aerosols and splatters

Figure 8 shows the size-resolved aerosol removal ratio by the commercial EOS at increasing distances. (1) *Airborne aerosols 1-10 μm* . For the suction velocity V of 6 m/s, the removal ratio slightly decreased from 97% to 85% and then sharply to around 11% when the distance was increased from 15 cm to 20 cm and then to 30 cm. For the V of 9 m/s, the removal ratio had a similar trend with the velocity of 6 m/s but with a higher value. Under V of 12 m/s, the removal ratios were higher than the lower velocities. However, the removal ratio was still low, with a value of 23% at a distance of 30 cm. (2) *Splatters 50-100 μm* . Under three suction velocities, the removal ratio of 50-100 μm splatters was around 76-83%, 40-64%, 17-61%, and 2-11% for the distance increase from 15 to 20 to 25 and 30 cm, respectively. Higher suction velocity resulted in a higher removal ratio of splatters. (3) *Droplets 500 μm* . For large droplets, the removal ratio decreased gradually from 18-20% to 5-10% as the distance increased from 15 cm to 30 cm. The removal ratio was almost independent of the suction velocity.

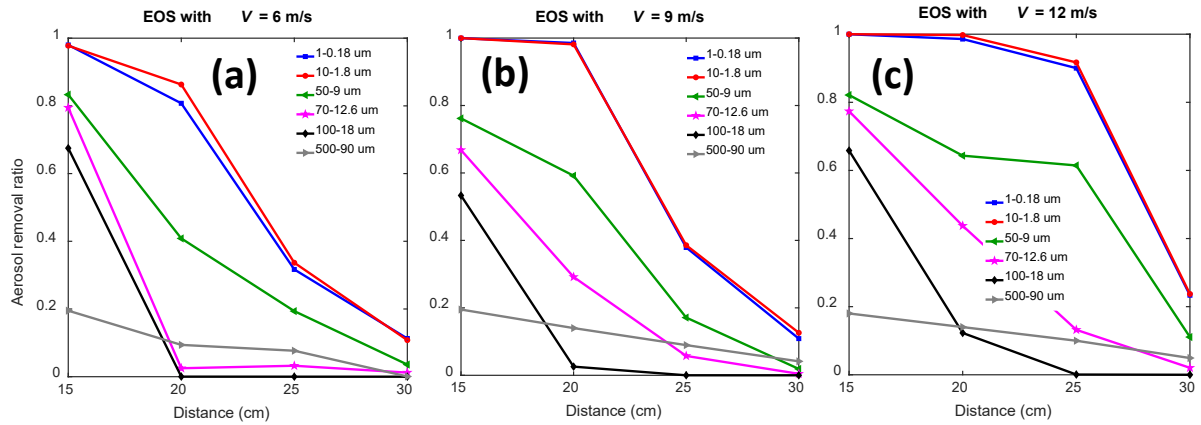


Figure 8. Aerosol removal ratio of the commercial EOS design at increasing distances under the suction velocity of (a) 6 m/s, (b) 9 m/s, and (c) 12 m/s. The legend format of "1-0.18 μm " indicated the initial and final diameters after complete evaporation.

The localized airflow path lines induced by the EOS are shown in Figure 9. For the distance of 15 cm, the path lines sank into the EOS head and covered the patient's mouth (Figure 9a). Therefore, the airborne aerosols followed the airflow and then were directly exhausted by the suction head with a removal ratio of up to 98% (Figure 10a). The splatters were either exhausted by the suction head or deposited on the patient's face (Figure 10b). Large droplets of 500 μm had enough inertia for a ballistic behavior independent of the airflow (Figure 10c). While at a distance of 30 cm, the path lines formed an anti-clockwise circulation (Figure 9b). However, the path lines above the patient's mouth did not sink into the suction head. Therefore, the airborne aerosols were carried horizontally downstream, and only a portion of the aerosols was exhausted (Figure 11a). The splatters moved downstream and deposited before the evaporation was finished due to the large gravitational force (Figure 11b). The large droplets had ballistic behavior and deposited on the nearby surfaces (Figure 11c).

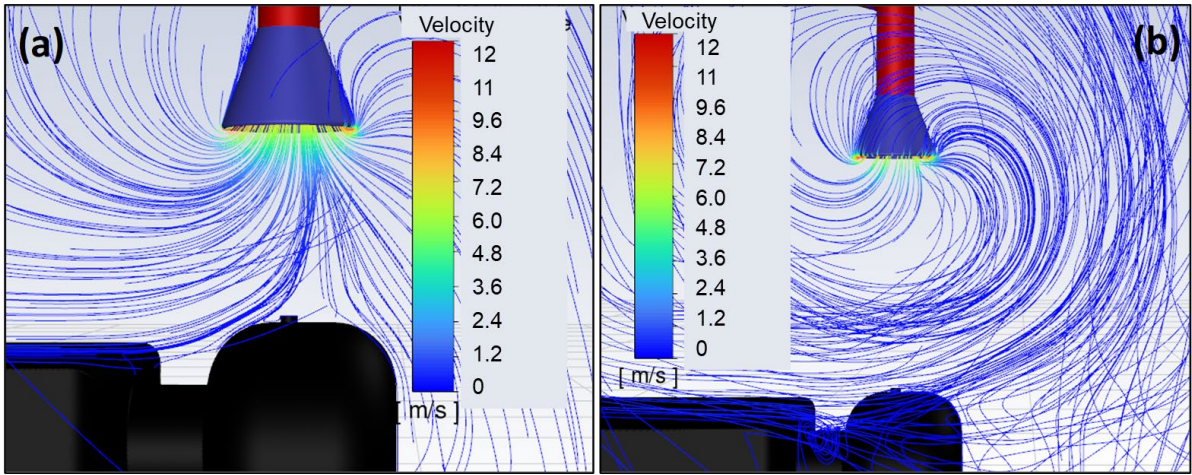


Figure 9. Airflow path lines induced by the traditional extraoral suction above the patient's face with the suction velocity of 12 m/s at a distance of (a) 15 cm and (b) 30 cm.

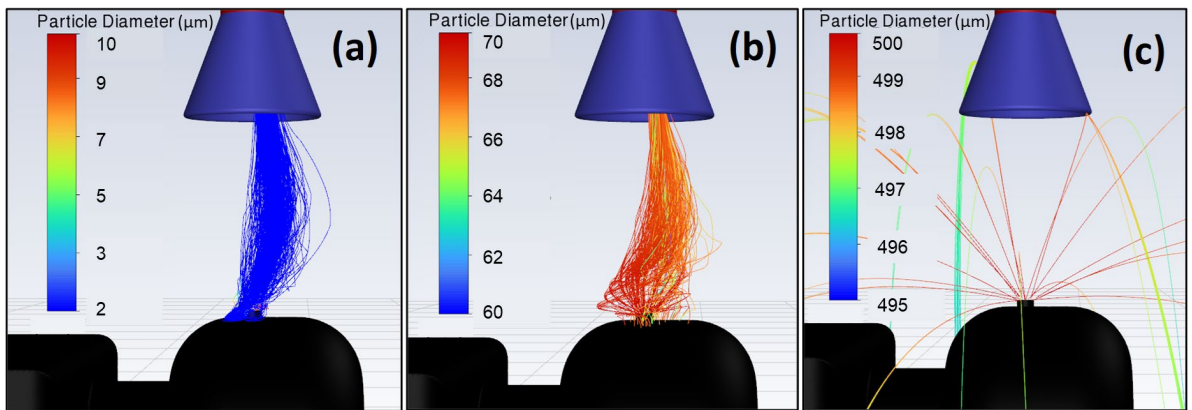


Figure 10. Trajectories of (a) aerosols of 10 μm , (b) splatters of 70 μm , and (c) droplets of 500 μm with a distance of 15 cm and suction velocity of 12 m/s. The legend indicated the size change due to evaporation.

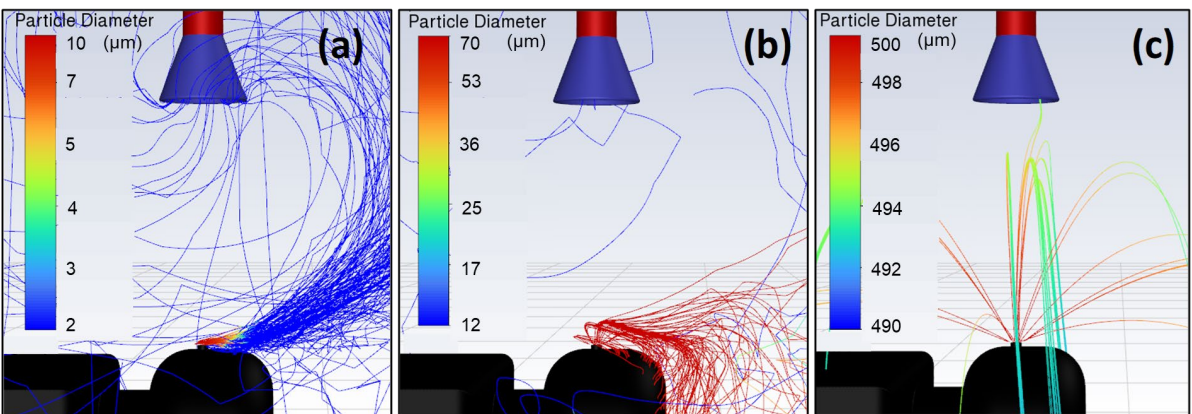


Figure 11. Trajectories of (a) aerosols of 10 μm , (b) splatters of 70 μm , and (c) droplets of 500 μm with a distance of 30 cm and suction velocity of 12 m/s. The legend indicated the size change due to evaporation.

Performance of the innovative EOS-AAC in removing dental aerosols and splatters

The aerosol removal ratios by the innovative EOS-AAC design at the distance of 30 cm are shown in Figure 12. The removal ratios of airborne aerosols were up to 98-99% for the different suction velocities V and air curtain velocities V_{AAC} , except for the V_{AAC} of 1 m/s under V of 6 m/s. The removal ratios of splatters were at the level of around 15%, which is independent of the suction velocity and air curtain velocity. The removal ratio of droplets increased as the air curtain velocity increased.

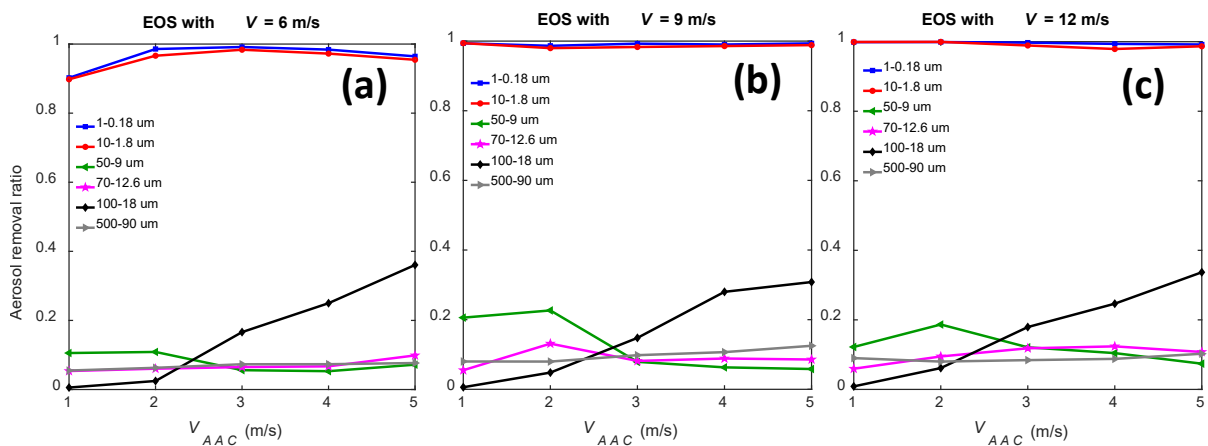


Figure 12. Aerosol removal ratio by the new EOS-AAC at the distance of 30 cm under the EOS velocity of (a) 6 m/s, (b) 9 m/s, and (c) 12 m/s.

The flow fields of the air curtain are shown in Figure 13. The air curtain directly pointed to the suction head, forming an isolated, enclosed area between the suction head and the patient head (Figure 13). An upward airflow below the AAC device was formed due to the air entrainment, which prevented the leakage of aerosols through the gap. The enclosed area became more robust as the air curtain and suction velocities increased. The airborne aerosols were confined inside the enclosed area (Figure 14a). The splatters were also confined inside the enclosed area,

but most were deposited on the patient's face with a small removal ratio by EOS (Figure 14b). The large droplets were not confined by the air curtain and deposited on nearby surfaces (Figure 14c).

The overall aerosols and splatters removed by EOS and immediately deposited on patient were not released outside the air curtain and had no harmful effect on the dentist. Therefore, the overall removal ratio by EOS and deposition on patients were summarized and shown in Figure 15. The removal ratio of splatters and airborne aerosols was up to 98-99%, except for the air curtain velocity 1 m/s under a suction velocity 6 m/s, indicating the excellent protection effect of the EOS-AAC. Large droplets' removal ratios were low, with a 20-30% value.

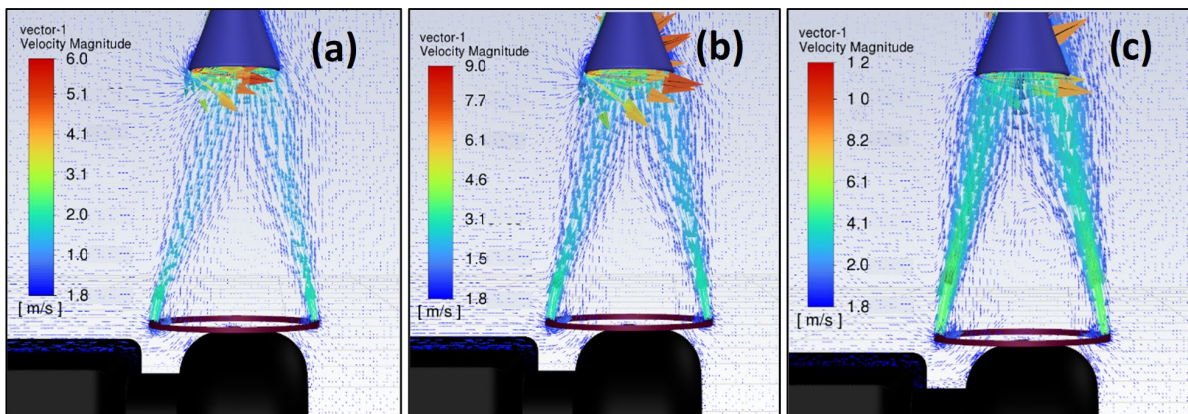


Figure 13. Airflow field above patient's face (a) EOS 6 m/s and V_{AAC} of 2 m/s, (b) EOS 9 m/s and V_{AAC} of 3 m/s, and (c) EOS 12 m/s and V_{AAC} of 5 m/s

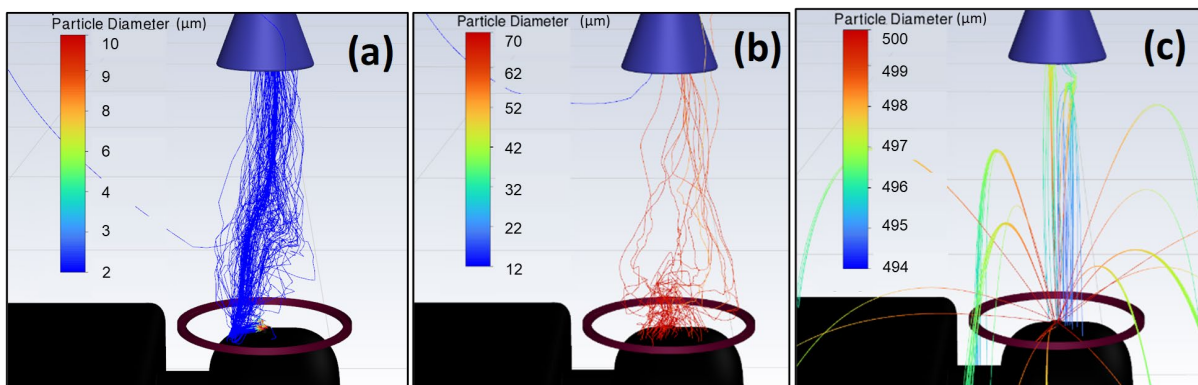


Figure 14. Trajectories of (a) aerosols of 10 μm , (b) splatters of 70 μm , and (c) droplets of 500 μm with EOS 6 m/s and the V_{AAC} of 2 m/s. The legend indicated the size change due to evaporation.

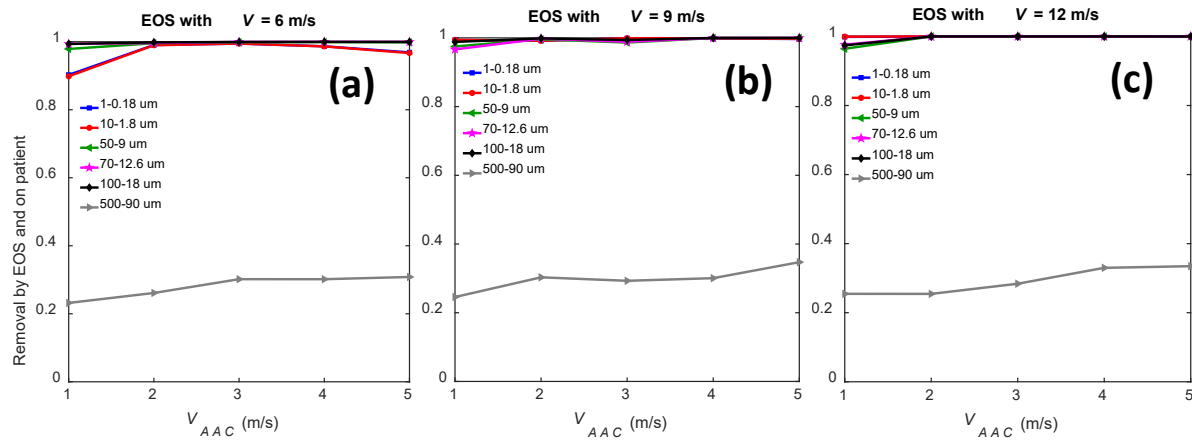


Figure 15. Aerosol removal ratio by the innovative EOS-AAC at a distance of 30 cm with increasing AAC velocity under the suction velocity of (a) 6 m/s, (b) 9 m/s, and (c) 12 m/s.

Robustness analysis of the innovative EOS-AAC

In this section, the robustness of the EOS-AAC was analyzed by considering the interaction of the AAC with the instrument and wrist, as shown in Figure 2c. All the studied cases of EOS of 6, 9, and 12 m/s and the AAC of 1, 2, 3, 4, and 5 m/s were considered in the robustness analysis. The removal ratio is shown in Figure 16. The EOS-AAC performed excellently in removing aerosols and splatters with 98% or higher removal ratios at the EOS-AAC velocities of 9-1, 9-2, 12-1, 12-2, and 12-3 m/s. Considering the robustness analysis, the performance of EOS-AAC was listed in Table 3 in different categories: Excellent, Good, Medium, and Bad. Under a constant EOS velocity, the performance was reduced as the AAC velocity increased. The higher air curtain velocity resulted in stronger interaction with the wrist/instrument, and more aerosols or splatters leaked outside of the enclosed area through the wrist or instrument surface. The performance was increased as the EOS velocity increased. The higher EOS velocity led to

stronger suction on the below air and aerosols. The Excellent category in Table 3 is suggested for the operational parameters of the EOS-AAC.

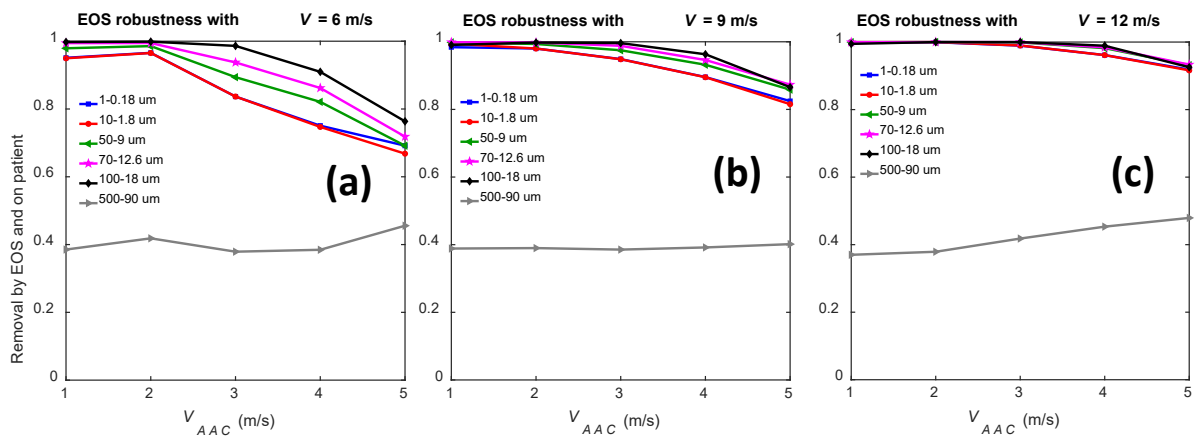


Figure 16. Robustness analysis of the removal ratio by EOS-AAC with EOS suction velocity of (a) 6 m/s, (b) 9 m/s, and (c) 12 m/s.

Table 3. Performance of EOS-AAC considering the robustness analysis

EOS-AAC	1 m/s	2 m/s	3 m/s	4 m/s	5 m/s
6 m/s	G	G	M	B	B
9 m/s	E	E	G	G	M
12 m/s	E	E	E	G	G

Note: E: excellent removal ratio > 98%; G: good removal ratio > 90%; M: medium removal ratio > 80%; B: bad removal ratio < 80%.

Discussion

Many works have characterized the performance of commercial EOS in dental clinics. The reduction ratios of aerosols and splatters in different studies were summarized in Table 3. During dental procedures, the reduction ratio ranges from 22% to 90% (> 100% for one research). The large discrepancy indicates that its performance is highly elusive. The methodologies, such as flow rates, positions, and measured parameters, were inconsistent

among different studies. The reduction ratios in previous studies partially reflect the efficacy of the extraoral suction. Our study found that the commercial EOS design only exhausts the immediately surrounding air. Therefore, only when the distance is within 20 cm will the EOS effectively remove most dental aerosols. For a more significant distance, the background airflow would mostly take dental aerosols and splatter away. It explains why the traditional EOS has a considerable variation of reduction ratios.

For the proposed design of EOS-AAC, the aerosol and splatter reduction ratios are stabilized at 98% or higher at a large distance of 30 cm, as summarized in Tables 3 and 4. The new EOS-AAC design performs much better than the commercial EOS design in removing aerosols and splatters. In addition, the axisymmetric AAC of the new design could block aerosols released in different directions. This can prevent dentists from continuously adjusting the suction head and be superior to the traditional design.

The new design can be used for common dental surgeries that generate many dental aerosols, such as ultrasonic scaling, high- and low-speed drilling, and tooth polishing. These dental surgeries generate over 80% in mass fraction of dental splatters smaller than 100 μm .⁵⁵ In addition, air turbine handpieces for drillings can generate more significant dental aerosols than other surgeries with a concentration of $\sim 200 \text{ \#/cm}^3$ and emission rate of $10^7 \text{ \# per minute}$,^{60, 63} which is comparative to the released particles in the simulation. The new EOS-AAC design has great potential to remove dental particles via a robust axisymmetric air curtain design.

After employing the EOS-AAC design to treat aerosol particles, dental splatters (50-100 μm) remain around the patient's face. This is because the splatters have more significant gravitational force than small aerosols, which deposit on the confined area by the air curtain instead of dispersing outside. For the traditional EOS, dental splatters quickly deposit on the nearby surface or are dispersed to the outside, which is affected by the airflow induced by EOS

and ventilation. Therefore, the EOS-AAC design has a much higher removal ratio for splatters than the traditional EOS design.

Table 4. The aerosol and splatter reduction ratios by EOS in references and this work

References	Reduction ratio
Teanpaisan et al. ⁶⁴	Mean counts of viable <i>E.coli</i> in aerosols were reduced from 29.26 to 17.26 CFU with a reduction ratio of 41%.
Junevičius et al. ³³	Splatter area ratios were reduced from 0.1%-10.0% to 0.02%-0.99% with a reduction ratio of around 90%.
Shahdad et al. ³⁹	20% reduction in frequency and a 75% reduction in concentration for the splatter around the operator.
Senpuku et al. ³⁴	Bacterial numbers falling around the dental chair were reduced from 46 to 36 with a reduction ratio of 22%
Horsophonphong et al. ⁴⁰	50% reduction of the total bacterial aerosols in the air and a 43% reduction in the splatter area.
Chavis et al. ⁴¹	Around 76% reduction of the average splatter area, located at 10 cm away from the patient's mouth with maximum flow rate
Graetz et al. ⁶⁵	Larger than 100% aerosol reduction at 35 cm away from patient's mouth. The aerosol concentration is lower than the background concentration after using the extraoral suction.
Commercial EOS design tested in this work	Aerosols: 98%-10% (distance 15 cm-30 cm); 99%-11%; 99%-23% for central suction velocity 6 m/s, 9 m/s, and 12 m/s. Splatters: 80%-0% (distance 15 cm-30 cm); 80%-0%; 80%-0% for velocity 6 m/s, 9 m/s, and 12 m/s.

The proposed new EOS-AAC design in this work	Aerosols and splatters: Above 98% for suction velocities of 9-12 m/s and air curtain velocities of 1–3 m/s under a large separation distance of 30 cm.
Efficiency improvement of EOS-AAC compared with EOS design	At the separation distance of 30 cm, the efficiency improvement for dental aerosols was 880%, 791%, and 326% for velocities of 6, 9, and 12 m/s, respectively. Efficiency improvement is calculated as the difference in removal ratios divided by the removal ratio of the EOS design.

In our field measurement at PPDH, the commercial EOS with the central velocity of 9, 11, and 12 m/s generated noise levels of 78, 83, and 84 dB near the patient and 73, 77, and 79 dB near the dentist. The significant noise is one crucial reason that prevents dentists from using an extraoral suction. The new design can achieve very high aerosol/splatter removal ratios with a low suction velocity of 6 m/s and air curtain velocity of 2 m/s, which will certainly reduce the noise level and help promote the use of the suction in more dental clinics.

Except for dental surgeries, this new design could also be promoted to the scenarios of point sources of contaminants requiring interactive operation, such as outpatients, surgeries for infected patients, etc. Furthermore, the annular air curtain technique can prevent the leakage of inner contaminants or protect the materials/targets from outside aerosols and pathogens.

Limitations

There are some limitations of this study. First, this work only numerically indicated the EOS-AAC design's high removal ratios of dental aerosols and splatters. The actual performance of the new design needs to be tested in practical dental surgeries via experimental studies. Second, the study of this work did not consider how to position the annular air curtain device above the

patient surface, which is a practical problem for applying EOS-AAC design in dental surgeries. Third, dental aerosols may have high concentrations for some surgeries, such as ultrasonic scaling and drilling using cooling water, leading to a higher possibility of aerosol coagulation and forming larger particles. The high concentration of aerosols also indicated the higher momentum of the aerosol plume, which may increase the leakage of the dental aerosols from the air curtain. Fourth, the relative humidity of the annular air curtain can affect the evaporation and dispersion of the confined dental aerosols and splatters. Only one relative humidity of the air curtain was considered in this work. Fifthly, only one setup of the annular air curtain was investigated. The annular air curtain's width, angle, and diameter also affect the dental aerosols' removal ratio, which needs further detailed studies. Finally, only one supplying angle of the air curtain was investigated at the fixed separation distance of 30 cm. The EOS-AAC design with more supplying angles and separation distances can be explored in the future.

Conclusions

Through this work, it is found that for a commercial EOS, the separation distance should be within 20 cm, and the central suction velocity should be 9-12 m/s (2.25-3 m³/min) to achieve a good aerosol removal ratio of 90% and splatter removal ratio of 20-60%. The patient's mouth area will be out of the influence area of the suction head if the separation distance is larger, which will lead to leakage of the dental aerosols to the main area with an aerosol removal ratio of 10%. However, the separation distance within 20 cm indicates the high possibility of obstructing dental surgeries by the EOS device. The proposed innovative EOS-AAC can achieve robust dental aerosol (< 50 μm) and splatter (50-100 μm) removal ratios of 98% at the separation distance of 30 cm. This is because the annual air curtain works as a virtual partition to confine the aerosols and splatters inside the small area without leakage. The virtual partition and the suction head create an upward airflow toward the suction head and remove the aerosols and splatters immediately. The new design can create large space for dental procedures and

reduce the noise by the lower suction velocity of 6 m/s and air curtain velocity of 1–3 m/s, compared with the higher velocity of 9-12 m/s for the commercial EOS design. The innovative design of the extraoral suction has great potential to create a clean dental environment and protect nearby dental professionals.

Acknowledgements

This work was supported by the General Research Fund (no. 17207121) from the Research Grants Council of the Hong Kong Special Administrative Region, China and the RAP Start-up Funds (P0033675 & P0043523) under the Strategic Hiring Scheme of The Hong Kong Polytechnic University.

Author Contributions

Wang: Conceptualization; Methodology; Formal analysis; Investigation; Writing – Original draft. Yang: Investigation; Software; Validation. Chao, Fu: Conceptualization; Supervision; Project administration. All authors approved the final version of the manuscript.

Declaration of competing interest

The authors have no competing interests to declare that are relevant to the content of this article.

References

1. Miller RL, Micik RE, Abel C and Ryge G. Studies on dental aerobiology: II. Microbial splatter discharged from the oral cavity of dental patients. *J Dent Res* 1971; 50: 621-625.
2. Micik RE, Miller RL, Mazarella MA and Ryge G. Studies on dental aerobiology: I. Bacterial aerosols generated during dental procedures. *J Dent Res* 1969; 48: 49-56.
3. Eklund K and Marianos D. Providing a safe environment for dental care in an era of infectious diseases. *J Am Dent Assoc* 2013; 144: 1330-1332.
4. Harrel SK and Molinari J. Aerosols and splatter in dentistry: a brief review of the literature and infection control implications. *J Am Dent Assoc* 2004; 135: 429-437.

5. Iliadi A, Koletsi D, Eliades T and Eliades G. Particulate production and composite dust during routine dental procedures. A systematic review with meta-analyses. *Materials* 2020; 13: 2513.
6. Leggat PA and Kedjarune U. Bacterial aerosols in the dental clinic: a review. *Int Dent J* 2001; 51: 39-44.
7. Zhu N, Zhang D, Wang W, Li X, Yang B, Song J, Zhao X, Huang B, Shi W and Lu R. A novel coronavirus from patients with pneumonia in China, 2019. *New Engl J Med* 2020; 382: 727-733.
8. Wang C, Horby PW, Hayden FG and Gao GF. A novel coronavirus outbreak of global health concern. *Lancet* 2020; 395: 470-473.
9. Allison JR, Currie CC, Edwards DC, Bowes C, Coulter J, Pickering K, Kozhevnikova E, Durham J, Nile CJ and Jakubovics N. Evaluating aerosol and splatter following dental procedures: Addressing new challenges for oral health care and rehabilitation. *J Oral Rehabil* 2021; 48: 61-72.
10. Allison JR, Currie CC, Edwards DC, Bowes C, Coulter J, Pickering K, Kozhevnikova E, Durham J, Nile CJ, Jakubovics N, Rostami N and Holliday R. 2020. DOI: 10.1101/2020.06.25.154401.
11. Kayahan E, Wu M, Van Gerven T, Braeken L, Stijven L, Politis C and Leblebici ME. Droplet size distribution, atomization mechanism and dynamics of dental aerosols. *J Aerosol Sci* 2022; 166: 106049.
12. Innes N, Johnson I, Al-Yaseen W, Harris R, Jones R, Kc S, McGregor S, Robertson M, Wade W and Gallagher JE. A systematic review of droplet and aerosol generation in dentistry. *J Dent* 2021; 105: 103556.
13. Adhikari A, Kurella S, Banerjee P and Mitra A. Aerosolized bacteria and microbial activity in dental clinics during cleaning procedures. *J Aerosol Sci* 2017; 114: 209-218.

14. Kobza J, Pastuszka J and Brągoszewska E. Do exposures to aerosols pose a risk to dental professionals? *Occup Med* 2018; 68: 454-458.
15. Bennett A, Fulford M, Walker J, Bradshaw D, Martin M and Marsh P. Microbial aerosols in general dental practice. *Br Dent J* 2000; 189: 664-667.
16. Grenier D. Quantitative analysis of bacterial aerosols in two different dental clinic environments. *Appl Environ Microbiol* 1995; 61: 3165-3168.
17. Rautemaa R, Nordberg A, Wuolijoki-Saaristo K and Meurman JH. Bacterial aerosols in dental practice—a potential hospital infection problem? *J Hosp Infect* 2006; 64: 76-81.
18. Wyllie AL, Fournier J, Casanovas-Massana A, Campbell M, Tokuyama M, Vijayakumar P, Geng B, Muenker MC, Moore AJ and Vogels CB. Saliva is more sensitive for SARS-CoV-2 detection in COVID-19 patients than nasopharyngeal swabs. *MedRxiv* 2020: 2020.2004.2016.20067835.
19. To KK-W, Tsang OT-Y, Yip CC-Y, Chan K-H, Wu T-C, Chan JM-C, Leung W-S, Chik TS-H, Choi CY-C and Kandamby DH. Consistent detection of 2019 novel coronavirus in saliva. *Clin Infect Dis* 2020; 71: 841-843.
20. Kutter JS, Spronken MI, Fraaij PL, Fouchier RA and Herfst S. Transmission routes of respiratory viruses among humans. *Curr Opin Virol* 2018; 28: 142-151.
21. Killingley B and Nguyen-Van-Tam J. Routes of influenza transmission. *Influenza Other Resp* 2013; 7: 42-51.
22. Li Y, Qian H, Hang J, Chen X, Cheng P, Ling H, Wang S, Liang P, Li J and Xiao S. Probable airborne transmission of SARS-CoV-2 in a poorly ventilated restaurant. *Build Environ* 2021; 196: 107788.
23. Jia W, Wei J, Cheng P, Wang Q and Li Y. Exposure and respiratory infection risk via the short-range airborne route. *Build Environ* 2022; 219: 109166.

24. Morawska L and Cao J. Airborne transmission of SARS-CoV-2: The world should face the reality. *Environ Int* 2020; 139: 105730.
25. Tang J, Li Y, Eames I, Chan P and Ridgway G. Factors involved in the aerosol transmission of infection and control of ventilation in healthcare premises. *J Hosp Infect* 2006; 64: 100-114.
26. Xie X, Li Y, Chwang A, Ho P and Seto W. How far droplets can move in indoor environments—revisiting the wells evaporation–falling curve. *Indoor Air* 2007; 17.
27. Sze-To GN, Yang Y, Kwan JK, Yu SC and Chao CY. Effects of surface material, ventilation, and human behavior on indirect contact transmission risk of respiratory infection. *Risk Anal* 2014; 34: 818-830.
28. Lei H, Li Y, Xiao S, Yang X, Lin C, Norris SL, Wei D, Hu Z and Ji S. Logistic growth of a surface contamination network and its role in disease spread. *Sci Rep* 2017; 7: 14826.
29. Wang P, Zhang N, Lee PK and Li Y. Quantification of *Lactobacillus delbrueckii* subsp. *bulgaricus* and its applicability as a tracer for studying contamination spread on environmental surfaces. *Build Environ* 2021; 197: 107869.
30. Meng L, Hua F and Bian Z. Coronavirus disease 2019 (COVID-19): emerging and future challenges for dental and oral medicine. *J Dent Res* 2020; 99: 481-487.
31. Peng X, Xu X, Li Y, Cheng L, Zhou X and Ren B. Transmission routes of 2019-nCoV and controls in dental practice. *Int J Oral Sci* 2020; 12: 1-6.
32. Remington WD, Ott BC and Hartka TR. Effectiveness of barrier devices, high-volume evacuators, and extraoral suction devices on reducing dental aerosols for the dental operator: A pilot study. *J Am Dent Assoc* 2022; 153: 309-318. e301.
33. Junevičius J, Šurna A and Šurna R. Effectiveness evaluation of different suction systems. *Stomatologija* 2005; 7: 52-57.

34. Senpuku H, Fukumoto M, Uchiyama T, Taguchi C, Suzuki I and Arikawa K. Effects of extraoral suction on droplets and aerosols for infection control practices. *Dent J* 2021; 9: 80.
35. Nulty A, Lefkaditis C, Zachrisson P, Van Tonder Q and Yar R. A clinical study measuring dental aerosols with and without a high-volume extraction device. *Br Dent J* 2020: 1-8.
36. Balanta-Melo J, Gutiérrez A, Sinisterra G, Díaz-Posso MdM, Gallego D, Villavicencio J and Contreras A. Rubber dam isolation and high-volume suction reduce ultrafine dental aerosol particles: an experiment in a simulated patient. *Appl Sci* 2020; 10: 6345.
37. Graetz C, Hülsbeck V, Düffert P, Schorr S, Straßburger M, Geiken A, Dörfer CE and Cyris M. Influence of flow rate and different size of suction cannulas on splatter contamination in dentistry: results of an exploratory study with a high-volume evacuation system. *Clin Oral Invest* 2022; 26: 5687-5696.
38. Suprono MS, Won J, Savignano R, Zhong Z, Ahmed A, Roque-Torres G, Zhang W, Oyoyo U, Richardson P and Caruso J. A clinical investigation of dental evacuation systems in reducing aerosols. *J Am Dent Assoc* 2021; 152: 455-462.
39. Shahdad S, Patel T, Hindocha A, Cagney N, Mueller J-D, Seoudi N, Morgan C and Din A. The efficacy of an extraoral scavenging device on reduction of splatter contamination during dental aerosol generating procedures: an exploratory study. *Br Dent J* 2020: 1-10.
40. Horsophonphong S, Chestsuttayangkul Y, Surarit R and Lertsooksawat W. Efficacy of extraoral suction devices in aerosol and splatter reduction during ultrasonic scaling: A laboratory investigation. *J Dent Res Dent Clin Dent Prospects* 2021; 15: 197.
41. Chavis SE, Hines SE, Dyalram D, Wilken NC and Dalby RN. Can extraoral suction units minimize droplet spatter during a simulated dental procedure? *J Am Dent Assoc* 2021; 152: 157-165.

42. Xu J, Guo H, Zhang Y and Lyu X. Effectiveness of personalized air curtain in reducing exposure to airborne cough droplets. *Build Environ* 2021; 108586.
43. Xu J, Wang C and Guo H. Effect of personalized air curtain combined with mixing ventilation on dispersion of aerosols released at different velocities from respiratory activities during close contact. *J Build Eng* 2024; 109016.
44. Liu S, Cao Q, Zhao X, Lu Z, Deng Z, Dong J, Lin X, Qing K, Zhang W and Chen Q. Improving indoor air quality and thermal comfort in residential kitchens with a new ventilation system. *Build Environ* 2020; 180: 107016.
45. Takamure K, Sakamoto Y, Yagi T, Iwatani Y, Amano H and Uchiyama T. Blocking effect of desktop air curtain on aerosols in exhaled breath. *AIP Adv* 2022; 12.
46. Chen M and Hao S. Numerical study on the cutting off performance of a novel personalized air curtain in a general consulting ward. *Dev Built Environ* 2023; 100239.
47. Ye J, Qian H, Ma J, Zhou R and Zheng X. Using air curtains to reduce short-range infection risk in consulting ward: A numerical investigation. In: *Build Simul* 2021, pp.325-335. Springer.
48. Rosa N, Gaspar A, Costa J, Lopes A, Pais JS and da Silva MG. Experimental assessment of an air curtain-sealed personal protective equipment for medical care: Influence of breathing and thermal plume. *Exp Therm Fluid Sci* 2023; 148: 110955.
49. Wei X, Yi D, Xie W, Gao J and Lv L. Protection against inhalation of gaseous contaminants in industrial environments by a personalized air curtain. *Build Environ* 2021; 206: 108343.
50. Ma J, Qian H, Liu F and Zheng X. Performance analysis of a novel personalized air curtain for preventing inhalation of particulate matters in industrial environments. *J Build Eng* 2022; 58: 105014.

51. Wei X, Xu Y, Ma M, Cao C, Niu G, Cao G and Gao J. Effect of ambient interferences on the effectiveness of a wearable ventilation for reducing pollutant exposure. *J Build Eng* 2023; 78. DOI: 10.1016/j.jobe.2023.107632.
52. Yang J-H, Cho H-S, Choi J, Hwang J and Lee J-H. A study on the structure of garment-hood-embedded air curtain with fine dust protection function. *Build Environ* 2023; 239: 110409.
53. Al Assaad D, Habchi C, Ghali K and Ghaddar N. Effectiveness of intermittent personalized ventilation in protecting occupant from indoor particles. *Build Environ* 2018; 128: 22-32.
54. Quadco. Water moisture content of humid air calculator, <https://www.quadco.engineering/en/know-how/cfd-calculate-water-fraction-humid-air.htm> (2023).
55. Xing C, Ai Z, Liu Z, Mak CM and Wong HM. Characteristics of droplets emission immediately around mouth during dental treatments. *Build Environ* 2024; 248: 111066.
56. Bergdahl M. Salivary flow and oral complaints in adult dental patients. *Community Dent Oral* 2000; 28: 59-66.
57. Navazesh M and Kumar SK. Measuring salivary flow: challenges and opportunities. *J Am Dent Assoc* 2008; 139: 35S-40S.
58. Von Fraunhofer J, Siegel S and Feldman S. Handpiece coolant flow rates and dental cutting. *Oper Dent* 2000; 25: 544-548.
59. Wang C, Xu J, Chan K, Lee H, Tso C, Lin CS, Chao CY and Fu S. Infection control measures for public transportation derived from the flow dynamics of obstructed cough jet. *J Aerosol Sci* 2022; 163: 105995.
60. Lahdentausta L, Sanmark E, Lauretsalo S, Korkee V, Nyman S, Atanasova N, Oksanen L, Zhao J, Hussein T and Hyvärinen A. Aerosol concentrations and size distributions during clinical dental procedures. *Heliyon* 2022; 8.

61. Xu Y, Yang X, Yang C and Srebric J. Contaminant dispersion with personal displacement ventilation, Part I: Base case study. *Build Environ* 2009; 44: 2121-2128.
62. Xu J, Guo H, Zhang Y and Lyu X. Effectiveness of personalized air curtain in reducing exposure to airborne cough droplets. *Build Environ* 2022; 208: 108586.
63. Rafiee A, Carvalho R, Lunardon D, Flores-Mir C, Major P, Quemerais B and Altabtbaei K. Particle size, mass concentration, and microbiota in dental aerosols. *J Dent Res* 2022; 101: 785-792.
64. Teanpaisan R, Taeporamaysamai M, Rattanachone P, Poldoung N and Srisintorn S. The usefulness of the modified extra-oral vacuum aspirator (EOVA) from household vacuum cleaner in reducing bacteria in dental aerosols. *I Den J* 2001; 51: 413-416.
65. Graetz C, Düffert P, Heidenreich R, Seidel M and Dörfer CE. The efficacy of an extraoral scavenging device on reducing aerosol particles $\leq 5 \mu\text{m}$ during dental aerosol-generating procedures: an exploratory pilot study in a university setting. *BDJ open* 2021; 7: 19.